BLOCK PRECONDITIONERS FOR THE MARKER-AND-CELL DISCRETIZATION OF THE STOKES–DARCY EQUATIONS*

CHEN GREIF† AND YUNHUI HE†

Abstract. We consider the problem of iteratively solving large and sparse double saddle-point systems arising from the stationary Stokes–Darcy equations in two dimensions, discretized by the Marker-and-Cell (MAC) finite difference method. We analyze the eigenvalue distribution of a few ideal block preconditioners. We then derive practical preconditioners that are based on approximations of Schur complements that arise in a block decomposition of the double saddle-point matrix. We show that including the interface conditions in the preconditioners is key in the pursuit of scalability. Numerical results show good convergence behavior of our preconditioned GMRES solver and demonstrate robustness of the proposed preconditioner with respect to the physical parameters of the problem.

Key words. Stokes–Darcy equations, Marker-and-Cell, double saddle-point systems, iterative solution, preconditioning, eigenvalues

AMS subject classifications. 65F08, 65F10, 65N06

1. Introduction. The numerical solution of coupled fluid problems has attracted a considerable attention of researchers and practitioners in the past few decades, in large part due to the importance of these problems and the computational challenges that they pose. The Stokes–Darcy model is an example of such a problem, and is the topic of this paper. The equations describe the flow of fluid across two subdomains: in one subdomain the fluid flows freely, and in the other it flows through a porous medium. The interface between the subdomains couples the two flow regimes and plays a central physical, mathematical, and computational role. It poses a challenge because the flow behaves significantly differently in terms of scale and other properties in each of the subdomains, and an abrupt change of scale may occur at the interface. There are several relevant applications of interest here: flow of water through sand and rock, flow of blood through arterial vessels, problems in hydrology, environment and climate science, and other applications; see, e.g., the comprehensive survey [14].

As far as the numerical solution of the equations is concerned, methods that solve the problem for the entire domain at once have been developed, as well as domain decomposition methods or iteration-by-subdomain methods, which solve separately the Stokes and the Darcy problems in an iterative fashion [15, 40, 29, 10, 9, 2, 36, 22, 27]. Different types of discretizations have been applied: finite element methods [26, 48, 12, 33, 5], finite difference/volume methods [41, 43, 31], and other methods [47, 18].

The Marker-and-Cell (MAC) scheme belongs to the class of finite difference methods, and is our focus in this work. MAC was proposed in [21] for the Stokes and Navier–Stokes equations. To achieve numerical stability, the scheme uses staggered grids in which the velocity and pressure are discretized at different locations of a grid cell. MAC has been used extensively for fluid flow problems, and a significant effort has been devoted to studying this scheme for Stokes–Darcy, the coupled Navier–

Stokes and Darcy flows [28], Stokes–Darcy–Brinkman equations [45], the compressible Stokes equations [17], and other multiphysics applications [30, 16]. A review of the Marker-and-Cell method can be found in [35].

As shown in [37, 34, 41] and several other references, the MAC scheme has a few advantages. It is well-tested and well-understood for standard fluid flow problems, and it allows for a relatively simple implementation. For the Stokes problem, it has been shown that the MAC scheme can be derived directly from a finite element method [20]. For the Navier–Stokes problem, MAC can be interpreted as a mixed finite element method of the velocity-vorticity variational formulation [19]. Recent papers prove numerical stability and convergence of the Stokes–Darcy equations [43, 45]. In this paper we use the discretization introduced in [43].

Preconditioners for GMRES for the Stokes–Darcy model discretized by the mixed finite element method have been proposed in [8]. In [13] an indefinite constraint preconditioner was studied. In [4] an augmented Lagrangian approach is used and a field-of-values analysis is performed. For multigrid solvers, the main challenge lies in designing effective smoothers for the coupled discrete systems. In [31], the authors develop an Uzawa smoother for the Stokes–Darcy problem discretized by finite volumes on staggered grids. The recent paper [32] provides an interesting description of some challenges that arise with various formuations of the problem. The authors show that standard preconditioning approaches based on natural norms are not parameter-robust, and they propose preconditioners that utilize non-standard and non-local operators, which are based on fractional derivatives. For additional useful references on solution approaches for solving the problem, see [42, 4].

In this work, we focus on preconditioning for the stationary Stokes–Darcy problem discretized by the MAC scheme. We propose block-structured preconditioners, perform a spectral analysis of the preconditioned operators, and show that they are suitable for preconditioned GMRES. Taking advantage of the sparsity structure of the matrix and using the coupling equations, we develop inexact approximations of the Schur complements and show that the iterative scheme is robust for a large range of the physical parameters.

In Section 2 we review the continuous Stokes–Darcy equations and in Section 3 we describe the MAC scheme for discretizing them. We develop block preconditioners and their inexact versions in Section 4. In Section 5 numerical results are presented. Finally, we draw some conclusions in Section 6.

2. Governing equations. We consider the coupled Stokes–Darcy problem in a two-dimensional domain comprised of two non-overlapping subdomains, $\Omega = \Omega_d \bigcup \Omega_s$; see Figure 1. In the bounded domain Ω_s we have a free fluid flow, and in Ω_d the flow is in a porous region. The flows are coupled across the interface Γ.

The Darcy equations in two dimensions for porous medium flow are given by

$$K^{-1}\boldsymbol{u}^d + \nabla p^d = 0 \quad \text{in } \Omega_d, \tag{2.1a}$$

$$\nabla \cdot \boldsymbol{u}^d = f^d \quad \text{in } \Omega_d, \tag{2.1b}$$

where $\boldsymbol{u}^d = (u^d, v^d)$ is the velocity and p^d is the fluid pressure inside the porous medium. K is the hydraulic (or permeability) tensor, representing the properties of the porous medium and the fluid. Throughout this paper we will assume $K = \kappa I$, where $\kappa > 0$ and I is the identity matrix. This amounts to treating the porous medium as homogeneous and isotropic, and we call κ the permeability constant.
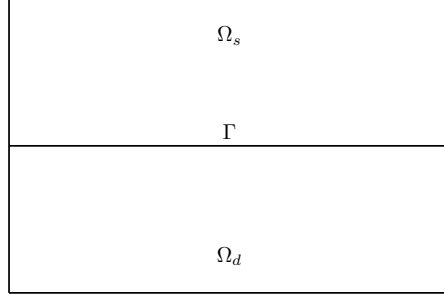
FIG. 1. *Two-dimensional domain for the Stokes–Darcy problem. The interface is marked by Γ.*

Denoting $\phi = p^d$ we combine (2.1a) and (2.1b) into

(2.2) $$-\nabla \cdot (\kappa \nabla \phi) = f^d \quad \text{in } \Omega_d.$$

The free-flow problem is described by the Stokes equations

(2.3a) $$-\nu \triangle \boldsymbol{u}^s + \nabla p^s = \boldsymbol{f}^s \quad \text{in } \Omega_s,$$

(2.3b) $$\nabla \cdot \boldsymbol{u}^s = 0 \quad \text{in } \Omega_s,$$

where $\boldsymbol{u}^s = (u^s, v^s)$ is the fluid velocity vector, p^s is the fluid pressure, and ν is the fluid viscosity.

Denoting $(\phi, \boldsymbol{u}, p) = (p^d, \boldsymbol{u}^s, p^s)$, Equations (2.2)–(2.3) give us the Stokes–Darcy problem in primal form:

(2.4a) $$-\kappa \triangle \phi = f^d \quad \text{in } \Omega_d,$$

(2.4b) $$-\nu \triangle \mathbf{u} + \nabla p = \boldsymbol{f}^s \quad \text{in } \Omega_s,$$

(2.4c) $$\nabla \cdot \mathbf{u} = 0 \quad \text{in } \Omega_s.$$

This is an alternative formulation to the one given by Equations (2.1) and (2.3), and we will focus from this point onward on this primal form. The problem is completed by setting interface conditions and imposing boundary conditions.

The interface conditions can be thought of as a boundary layer through which the velocity changes rapidly. The following three interface conditions are often used to couple the Darcy and Stokes equations at the interface Γ:

(2.5a) $$v = -\kappa \frac{\partial \phi}{\partial y};$$

(2.5b) $$p - \phi = 2\nu \frac{\partial v}{\partial y};$$

(2.5c) $$u = \frac{\nu}{\alpha} \left(\frac{\partial u}{\partial y} + \frac{\partial v}{\partial x} \right).$$

Equation (2.5a) is a *mass conservation condition*, and it guarantees continuity of normal velocity components. Equation (2.5b) is a condition on the *balance of normal forces*, and it allows the pressure to be discontinuous across the interface. Finally, (2.5c), the *Beavers-Joseph-Saffman condition*, provides a suitable slip condition on the tangential velocity.

119   The physical and mathematical properties associated with the interface conditions
120 have been extensively studied in the literature; see, e.g., [46, 24]. A central challenge
121 in the solution of the Stokes–Darcy equations is that the equations governing each
122 domain are fundamentally different. This difficulty is manifested especially when the
123 parameters involved, specifically the viscosity coefficient ν and permeability constant
124 κ, differ from each other by a few orders of magnitude.

125   **3. Discretization.** The Marker-and-Cell scheme [35, 17] is an established and
126 popular discretization technique that has been extensively used in the solution of
127 fluid flow problems [45, 41, 43]. The components of the velocity and the pressure
128 are discretized at different locations on the grid, in a way that aims at accomplishing
129 numerical stability. Figure 2 shows the location of the discrete variables for (2.2)–
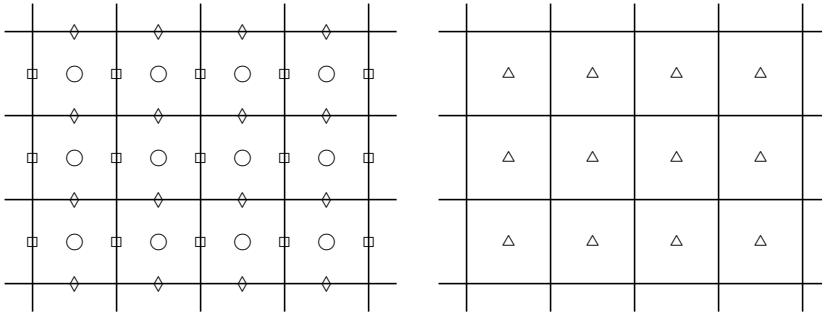130 (2.3).

FIG. 2. *The locations of the unknowns on the staggered grids. Left: the Stokes variables:* $\square$ – *u,* $\diamond$ – *v,* $\bigcirc$ – *p; Right: the Darcy variable:* $\triangle$ – ϕ.

131   The stability and convergence order of the MAC discretization for the Stokes–
132 Darcy equations have been established in the literature. In [43], a MAC scheme is
133 developed and a stability analysis is performed for the velocity and the pressure, and
134 error estimates are given for uniform grids. Let the two subdomains have the same
135 length, L, in the y direction. By [43, Theorem 4.1], if the meshsize h satisfies

136 (3.1) $$h \leqslant \min\left\{\frac{\nu\kappa}{2L}, \frac{2\alpha}{L}\right\},$$

137 then first-order convergence is guaranteed. In some of the tests in that paper second-
138 order convergence was in fact experimentally observed. Our discretization follows
139 the discretization of [43]. In Section 5 we provide a brief experimental study of
140 convergence order. We note that in [41] the authors use a finite volume technique
141 for the tensor format of the fluid operator near the interface and prove that under
142 the assumption that the solution is sufficiently smooth, second-order convergence is
143 obtained in the L_2-norm for both velocity and pressure of the Stokes and Darcy flows.

  3.1. Discretization at interior gridpoints for Stokes. Suppose the Stokes
domain is given by $[x^s_{\min}, x^s_{\max}] \times [y^s_{\min}, y^s_{\max}]$, with $x^s_{\max} - x^s_{\min} = y^s_{\max} - y^s_{\min}$. We
consider a uniform mesh with $n + 1$ gridpoints in each direction, yielding meshsize

$$h = \frac{x^s_{\max} - x^s_{\min}}{n} = \frac{y^s_{\max} - y^s_{\min}}{n}.$$

144   For simplicity, throughout we assume that the Stokes and the Darcy domains are
145 both square and are of the same size. We assign double subscripts to the gridpoints,
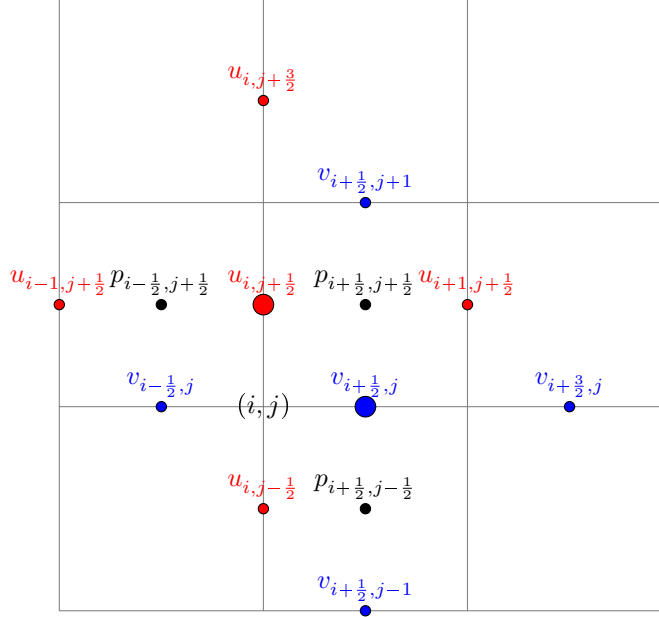
Fig. 3. *Discretization of interior gridpoints for the Stokes equations. The gridpoints about which the discretizations are given are marked with bigger circles. The red circles mark u variables and the blue circles mark v variables. The black circles denote pressure.*

which mark their locations on the grid. Throughout we will assume that, for a function $f(x,y)$ for example, a value written as $f_{i,j}$ corresponds to an approximation or an exact evaluation of the function at $x = ih$ and $y = jh$. The same applies for a 'half index.' Here, let us highlight the different locations of the grid where the discretization takes place. Given a double index (i, j), in the MAC configuration the discrete solution for the corresponding u variable is denoted as $u_{i,j+\frac{1}{2}}$, and for the corresponding v variable it is denoted as $v_{i+\frac{1}{2},j}$. Figure 3 provides a schematic illustration of the discretization for the interior variables.

To further describe the discretization, it is useful to write the Stokes momentum equation (2.4b) in scalar form:

(3.2)
$$\begin{cases} -\nu \left(\dfrac{\partial^2 u}{\partial x^2} + \dfrac{\partial^2 u}{\partial y^2} \right) + \dfrac{\partial p}{\partial x} = f_1^s, \\ -\nu \left(\dfrac{\partial^2 v}{\partial x^2} + \dfrac{\partial^2 v}{\partial y^2} \right) + \dfrac{\partial p}{\partial y} = f_2^s, \end{cases}$$

where $f_i^s, i = 1, 2$ denote the vector-components of $\boldsymbol{f}^s$ corresponding to the velocity components u and v. Using centered differences for the first and second derivatives, the corresponding discretization for the first equation in (3.2) at gridpoint $(ih, (j+\frac{1}{2})h)$ is given by

$$-\nu \left(\frac{u_{i+1,j+\frac{1}{2}} + u_{i-1,j+\frac{1}{2}} + u_{i,j+\frac{3}{2}} + u_{i,j-\frac{1}{2}} - 4u_{i,j+\frac{1}{2}}}{h^2} \right) + \frac{p_{i+\frac{1}{2},j+\frac{1}{2}} - p_{i-\frac{1}{2},j+\frac{1}{2}}}{h} = (f_1^s)_{i,j+\frac{1}{2}},$$

whereas the discretization for the second equation in (3.2) at gridpoint $((i + \frac{1}{2})h, jh)$

163   is

164    $$-\nu\left(\frac{v_{i+\frac{1}{2},j+1} + v_{i+\frac{1}{2},j-1} + v_{i+\frac{3}{2},j} + v_{i-\frac{1}{2},j} - 4v_{i+\frac{1}{2},j}}{h^2}\right) + \frac{p_{i+\frac{1}{2},j+\frac{1}{2}} - p_{i+\frac{1}{2},j-\frac{1}{2}}}{h} = (f_2^s)_{i+\frac{1}{2},j}.$$

165   Given the staggered grid configuration, we have $n(n-1)$ gridpoints for u and the
166   same number for v, but the internal indexing is different between those two velocity
167   components. For the u variables, the interior gridpoints correspond to $(x_i, y_{j+\frac{1}{2}}), 1 \leqslant$
168    $i \leqslant n-1, 0 \leqslant j \leqslant n-1$, and for the v variables the interior gridpoints correspond to
169    $(x_{i+\frac{1}{2}}, y_j), 0 \leqslant i \leqslant n-1, 1 \leqslant j \leqslant n-1$.

   Boundary conditions. If Dirichlet boundary conditions are given, the values for
the u gridpoints are prescribed for the vertical boundary points corresponding to $i = 0$
and $i = n$. For the horizontal boundary values corresponding to the u variables, since
the discrete values closest to the top boundary, i.e., with respect to $j = n$, appear as
$u_{i,n-\frac{1}{2}}, 1 \leqslant i \leqslant n-1$, and are not right on the boundary, we define ghost variables
$u_{i,n+\frac{1}{2}}, 1 \leqslant i \leqslant n-1$, and use an average

$$u_{i,n} = \frac{u_{i,n-\frac{1}{2}} + u_{i,n+\frac{1}{2}}}{2}$$

170   to assign the boundary conditions. It follows that $u_{i,n+\frac{1}{2}} = 2u_{i,n} - u_{i,n-\frac{1}{2}}$, which is
171   used in the discrete Stokes equations for $u_{i,n-\frac{1}{2}}$. This follows a standard approach;
172   see, for example, [11]. The points near $j = 0$ are treated separately as part of the
173   interface conditions; see Section 3.3.

   As for the v variables, for $j = 0$ see Section 3.3, which describes the interface
conditions. For $j = n$ the Dirichlet boundary conditions are prescribed directly. For
the discrete values $v_{\frac{1}{2},j}$ and $v_{n-\frac{1}{2},j}, 1 \leqslant j \leqslant n-1$, we use averages

$$v_{0,j} = \frac{v_{-\frac{1}{2},j} + v_{\frac{1}{2},j}}{2} \quad \text{and} \quad v_{n,j} = \frac{v_{n-\frac{1}{2},j} + v_{n+\frac{1}{2},j}}{2}$$

174   respectively, from which we extract the ghost variables $v_{-\frac{1}{2},j}$ and $v_{n+\frac{1}{2},j}$ and substi-
175   tute them in the discrete Stokes equations, analogously to the u variables.
176   For example, the discretization of the second equation in (3.2) at gridpoint $(\frac{1}{2}h, h)$
177   is given by

178    $$-\nu\frac{v_{-\frac{1}{2},1} + v_{\frac{3}{2},1} + v_{\frac{1}{2},0} + v_{\frac{1}{2},2} - 4v_{\frac{1}{2},1}}{h^2} + \frac{p_{\frac{1}{2},\frac{3}{2}} - p_{\frac{1}{2},\frac{1}{2}}}{h} = (f_2^s)_{\frac{1}{2},1},$$

179   where $v_{-\frac{1}{2},1}$ is a ghost variable, which can be eliminated by the linear extrapolation
180    $(v_{-\frac{1}{2},1} + v_{\frac{1}{2},1})/2 = v_{0,1} \equiv v_D(0,h)$, the given Dirichlet boundary condition. Using this
181   equation to eliminate the ghost variable, we obtain

182   (3.3) $$-\nu\frac{v_{\frac{3}{2},1} + v_{\frac{1}{2},0} + v_{\frac{1}{2},2} - 5v_{\frac{1}{2},1}}{h^2} + \frac{p_{\frac{1}{2},\frac{3}{2}} - p_{\frac{1}{2},\frac{1}{2}}}{h} = (f_2^s)_{\frac{1}{2},1} + \frac{2\nu v_{0,1}}{h^2}.$$

3.2. Discretization at interior gridpoints for Darcy. The discretization
for the Darcy variable, ϕ, is simpler than the discretization for Stokes. Here we
work on Ω_d. The Darcy domain is given by $[x_{\min}^d, x_{\max}^d] \times [y_{\min}^d, y_{\max}^d]$. We assume
$x_{\max}^d - x_{\min}^d = y_{\max}^d - y_{\min}^d$ and consider a uniform mesh with meshsize h, similarly to
the Stokes subdomain (for simplicity we will assume throughout that the Stokes and
the Darcy meshsizes are equal):

$$h = \frac{x_{\max}^d - x_{\min}^d}{n} = \frac{y_{\max}^d - y_{\min}^d}{n}.$$
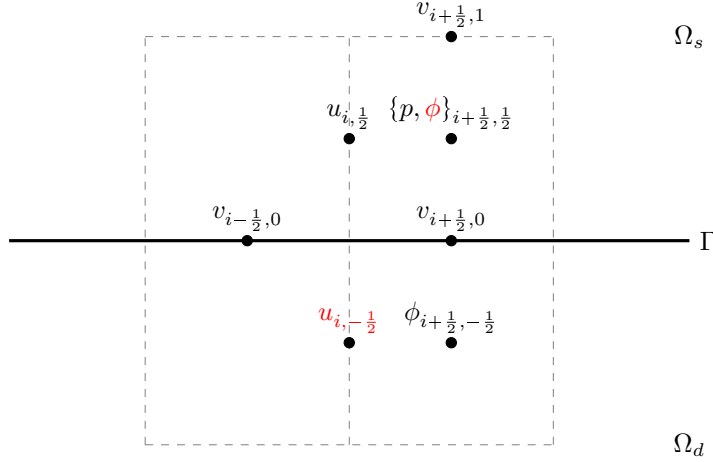
Fig. 4. *Discretization of the variables near the interface. The ghost variables that are to be eliminated are marked in red.*

We assign negative grid indices for the y variables: $-n \leqslant j \leqslant 0$. At the gridpoint $((i + \frac{1}{2})h, (j + \frac{1}{2})h)$, the discretization for (2.4a) is given by

$$-\kappa \left(\frac{\phi_{i+\frac{1}{2},j-\frac{1}{2}} + \phi_{i+\frac{1}{2},j+\frac{3}{2}} + \phi_{i+\frac{3}{2},j+\frac{1}{2}} + \phi_{i-\frac{1}{2},j+\frac{1}{2}} - 4\phi_{i+\frac{1}{2},j+\frac{1}{2}}}{h^2} \right) = (f^d)_{i+\frac{1}{2},j+\frac{1}{2}}.$$

3.3. Discretization of interface conditions. The interface conditions (2.5) present a few challenges. We use ghost variable to discretize our variables, as illustrated in Figure 4. There is a significant difference between the way the u variables and the v variables are handled on the interface. This is because the discrete v variables lie precisely on the interface, whereas the discrete u variables do not.

Following [43], the interface conditions are discretized as follows. For $1 \leqslant i \leqslant n-1$:

- mass conservation, $v = -\kappa \frac{\partial \phi}{\partial y}$:

$$(3.4) \qquad v_{i+\frac{1}{2},0} = -\kappa \frac{\phi_{i+\frac{1}{2},\frac{1}{2}} - \phi_{i+\frac{1}{2},-\frac{1}{2}}}{h};$$

- balance of normal forces, $p - \phi = 2\nu \frac{\partial v}{\partial y}$:

$$(3.5) \qquad p_{i+\frac{1}{2},\frac{1}{2}} - \phi_{i+\frac{1}{2},-\frac{1}{2}} = 2\nu \frac{v_{i+\frac{1}{2},1} - v_{i+\frac{1}{2},0}}{h};$$

- Beavers-Joseph-Saffman (BJS) condition, $u = \frac{\nu}{\alpha} \left(\frac{\partial u}{\partial y} + \frac{\partial v}{\partial x} \right)$:

$$(3.6) \qquad \frac{u_{i,\frac{1}{2}} + u_{i,-\frac{1}{2}}}{2} = \frac{\nu}{\alpha} \left(\frac{u_{i,\frac{1}{2}} - u_{i,-\frac{1}{2}}}{h} + \frac{v_{i+\frac{1}{2},0} - v_{i-\frac{1}{2},0}}{h} \right).$$

Equations (3.4)–(3.6) are coupled with the discretized Stokes and Darcy equations. The discretized Darcy equations for $\phi_{i+\frac{1}{2},-\frac{1}{2}}$ involve the ghost values, $\phi_{i+\frac{1}{2},\frac{1}{2}}$, which can be eliminated using (3.4).

The discretized equations for interface variables $v_{i+\frac{1}{2},0}$ are formed using (3.5). The discretized Stokes equations for the $u_{i,\frac{1}{2}}$ variables involve the ghost values, $u_{i,-\frac{1}{2}}$, which can be eliminated using (3.6).

3.4. The linear system. Putting together the equations for the interior grid-points and the interface conditions and incorporating boundary conditions, we obtain a double saddle-point system of the form

(3.7)
$$\begin{pmatrix} A_d & -G^T & 0 \\ G & A_s & B^T \\ 0 & B & 0 \end{pmatrix} \begin{pmatrix} \phi_h \\ \boldsymbol{u}_h \\ p_h \end{pmatrix} = \begin{pmatrix} g_1 \\ \boldsymbol{g}_2 \\ g_3 \end{pmatrix},$$

where A_d corresponds to $-\kappa\triangle$ for the Darcy equation and $A_s (\neq A_s^T)$ is the discretization of $-\nu\triangle$ for the Stokes equations coupled with the discretized interface conditions. The last block row in (3.7) corresponds to the (negated) divergence-free condition. Due to the boundary and interface conditions, the coefficient matrix in (3.7) is nonsymmetric. Double saddle-point systems of a similar form have been extensively studied recently [6, 23, 8], but the focus has mainly been on symmetric instances. In this paper we offer new insights into the nonsymmetric case.

The linear system (3.7) has $4n^2 - n$ unknowns, and we have $A_d \in \mathbb{R}^{n^2 \times n^2}$, $A_s \in \mathbb{R}^{(2n^2-n) \times (2n^2-n)}$, $G \in \mathbb{R}^{(2n^2-n) \times n^2}$, and $B \in \mathbb{R}^{n^2 \times n^2}$. In the sequel we describe the structure of the submatrices of (3.7). To avoid ambiguity when it may arise, when necessary we attach subscripts to identity matrices to indicate their sizes.

The matrix A_d. The matrix A_d can be naturally partitioned as a 2×2 block matrix having the following structure:

(3.8)
$$A_d = \begin{pmatrix} A_{d,11} & A_{d,12} \\ A_{d,21} & A_{d,22} \end{pmatrix}, \quad A_d = A_d^T, \quad A_{d,12} = A_{d,21}^T,$$

where $A_{d,11} \in \mathbb{R}^{(n^2-n) \times (n^2-n)}$, $A_{d,21} \in \mathbb{R}^{n \times (n^2-n)}$, $A_{d,22} \in \mathbb{R}^{n \times n}$, and

$$A_{d,21} = -\frac{\kappa}{h^2} \begin{pmatrix} 0 & I_n \end{pmatrix}.$$

The second block row of A_d, namely $(A_{d,21} \ A_{d,22})$, corresponds to the discrete n equations for ϕ near the interface Γ, and it is coupled with the discrete interface variables v, which appear in G^T; see (3.7).

The matrix A_s. The matrix A_s is a 3×3 block matrix with the structure

(3.9)
$$A_s = \begin{pmatrix} A_{11} & A_{12} & 0 \\ 0 & A_{22} & A_{23} \\ 0 & A_{32} & A_{33} \end{pmatrix};$$

Figure 5 depicts the dimensions of the blocks.

The matrix A_{12} is $(n^2 - n) \times n$, as can be inferred from Figure 5, and it is mostly zero. It is comprised of an $(n-1) \times n$ upper bidiagonal block stacked on top of an $(n^2 - 2n + 1) \times n$ zero block. The bidiagonal block is given by $c \cdot \mathrm{bidiag}[1, -1]$, where $c = \frac{2\nu^2}{h^2(2\nu+h\alpha)}$. This matrix represents the discretization of the discrete function values $u_{i,\frac{1}{2}}$, $1 \leqslant i \leqslant n-1$, which interact with the interface variables $v_{i+\frac{1}{2},0}$, using (3.6).

The matrix A_{22}, which corresponds to the interface v variables, has dimensions $n \times n$ and a simple structure: it is equal to a scaled identity matrix with $\frac{2\nu}{h^2}$.

The blocks of A_s satisfy $A_{11} = A_{11}^T, A_{22} = A_{22}^T, A_{33} = A_{33}^T$, and

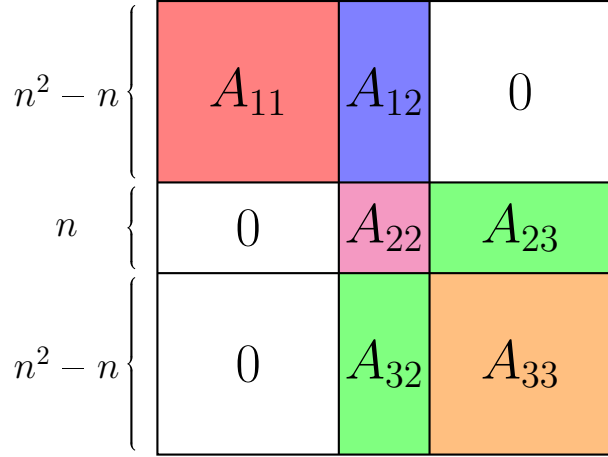$$A_{22} = \frac{2\nu}{h^2} I_n, \quad A_{23} = (-A_{22}, \ 0), \quad A_{32} = \frac{1}{2} A_{23}^T.$$

FIG. 5. *Block structure of A_s.*

Notice that while both A_{11} and A_{33} are $(n^2 - n) \times (n^2 - n)$, their internal block structures are different, due to the staggered grid. The matrix A_{11} (which corresponds to the u variables) is block tridiagonal with n blocks of dimensions $(n-1) \times (n-1)$, whereas A_{33} (which corresponds to the v variables) is block tridiagonal with $n-1$ blocks of dimensions $n \times n$ each.

The coupling matrix G. The equations for the $u_{i,\frac{1}{2}}$ variables are coupled with the discrete interface variables $v_{i+\frac{1}{2},0}$, which are represented by the matrix G in (3.7). G^T is a 2×3 block matrix with the following attractively simple structure:

(3.10)
$$G^T = \begin{pmatrix} 0 & 0 & 0 \\ 0 & -I_n/h & 0 \end{pmatrix}.$$

The nonzero block arises from the discretization of $\phi_{i+\frac{1}{2},-\frac{1}{2}}$, using (3.4).

The matrix B. The matrix B is a standard discrete divergence operator given by

(3.11) $\quad B = \begin{pmatrix} B_x & B_0 & B_y \end{pmatrix} \in \mathbb{R}^{n^2 \times (2n^2 - n)}, \quad B_0 = \begin{pmatrix} I_n/h \\ 0 \end{pmatrix} \in \mathbb{R}^{n^2 \times n}.$

Dirichlet boundary conditions are given by

$$\boldsymbol{u}^s = g_D^s \quad \text{on } \partial\Omega_s,$$
$$\phi = g_D^d \quad \text{on } \partial\Omega_d.$$

Neumann or mixed boundary conditions are also commonly considered; see, for example, [31, 41, 43] and the references therein.

3.5. Properties of the matrices. Let us rewrite the linear system (3.7) in a form that symmetrizes the off-diagonal blocks:

$$\begin{pmatrix} A_d & G^T & 0 \\ G & -A_s & B^T \\ 0 & B & 0 \end{pmatrix} \begin{pmatrix} \phi_h \\ -\boldsymbol{u}_h \\ p_h \end{pmatrix} = \begin{pmatrix} g_1 \\ \boldsymbol{g}_2 \\ -g_3 \end{pmatrix}.$$

Let

$$\mathcal{K} = \begin{pmatrix} A_d & G^T & 0 \\ G & -A_s & B^T \\ 0 & B & 0 \end{pmatrix}.$$

(3.13)

The blocks of $\mathcal{K}$ satisfy a few useful properties.

1. A_s is nonsymmetric and positive definite.
2. $(G \quad B^T)$ has a one-dimensional null space spanned by an all-ones vector of size $2n^2$.
3. B has full rank.
4. If we consider Neumann boundary conditions for the Darcy problem, then A_d is symmetric positive semidefinite with a one-dimensional null space spanned by all-ones vector. $\mathcal{K}$ is nonsymmetric and singular with a one-dimensional null space spanned by $\begin{pmatrix} e \\ 0 \\ e \end{pmatrix}$, where e is the vector of all ones of length n^2 and 0 is the zero vector of length $2n^2 - n$.
5. If we consider Dirichlet boundary conditions for the Darcy problem, then A_d is symmetric positive definite, and $\mathcal{K}$ is nonsymmetric and nonsingular.

For simplicity, in this paper we consider Dirichlet boundary conditions.

LEMMA 3.1. *All eigenvalues of A_s, which represents the Stokes equations and interface equations and is given in* (3.9), *are positive.*

Proof. The eigenvalues of A_s are a union of the eigenvalues of A_{11} and

$$E = \begin{pmatrix} A_{22} & A_{23} \\ A_{32} & A_{33} \end{pmatrix} = \begin{pmatrix} A_{22} & 2A_{32}^T \\ A_{32} & A_{33} \end{pmatrix}.$$

The matrix E is symmetrizable by a diagonal matrix $\tilde{D} = \begin{pmatrix} I_n & 0 \\ 0 & \sqrt{2}I_{n^2-n} \end{pmatrix}$, and therefore its eigenvalues are real. Since A_{11} is symmetric and diagonally dominant with positive elements on its diagonal, its eigenvalues are positive.

Let $\tilde{A}_{32} = \sqrt{2}A_{32}$. The block LDL^T decomposition of $\tilde{E} = \tilde{D}E\tilde{D}^{-1}$ is

$$\tilde{E} = \begin{pmatrix} A_{22} & \tilde{A}_{32}^T \\ \tilde{A}_{32} & A_{33} \end{pmatrix} = \begin{pmatrix} I_n & 0 \\ \tilde{A}_{32}A_{22}^{-1} & I_{n^2-n} \end{pmatrix} \begin{pmatrix} A_{22} & 0 \\ 0 & A_{33} - \tilde{A}_{32}A_{22}^{-1}\tilde{A}_{32}^T \end{pmatrix} \begin{pmatrix} I_n & A_{22}^{-1}\tilde{A}_{32}^T \\ 0 & I_{n^2-n} \end{pmatrix}.$$

A simple calculation shows that

$$A_{33} - \tilde{A}_{32}A_{22}^{-1}\tilde{A}_{32}^T = A_{33} - \frac{1}{2}(-A_{22} \ 0)^T A_{22}^{-1}(-A_{22} \ 0)$$

$$= A_{33} - \begin{pmatrix} \frac{\nu}{h^2}I_n & 0 \\ 0 & 0 \end{pmatrix}.$$

Thus, the above matrix is the same as A_{33} except the top left $n \times n$ block, and we now discuss the structure of that specific block of A_{33}.

The first and nth rows of A_{33} have three nonzero elements $[-\nu/h^2, 5\nu/h^2, -\nu/h^2]$, where the value 5 is due to Dirichlet boundary conditions; see (3.3). Rows 2 to $n-1$ have four nonzero elements $[-\nu/h^2, 4\nu/h^2, -\nu/h^2, -\nu/h^2]$, where the positive values are located at the diagonal position and we have diagonal dominance here. It follows that all eigenvalues of A_s are positive, as required. $\qquad\square$

Next, we state a rank property of B, which will be used later in our spectral analysis. The proof is omitted.

LEMMA 3.2. *Define*

(3.14)
$$\bar{B} = \begin{pmatrix} B_x & B_y \end{pmatrix} \in \mathbb{R}^{n^2 \times m_2},$$

where $m_2 = (2n^2 - n) - n = 2n^2 - 2n$. *Then,* $\operatorname{rank}(\bar{B}) = n^2 - 1$ *and the nullity of* $\bar{B}$ *is* $(n-1)^2$.

4. Block preconditioners. Block factorizations of the double saddle-point matrix $\mathcal{K}$ defined in (3.13) motivate the derivation of potential preconditioners. We write

(4.1)
$$\begin{pmatrix} A_d & G^T & 0 \\ G & -A_s & B^T \\ 0 & B & 0 \end{pmatrix} = \underbrace{\begin{pmatrix} I & 0 & 0 \\ GA_d^{-1} & I & 0 \\ 0 & -BS_1^{-1} & I \end{pmatrix}}_{L} \underbrace{\begin{pmatrix} A_d & 0 & 0 \\ 0 & -S_1 & 0 \\ 0 & 0 & S_2 \end{pmatrix}}_{D} \underbrace{\begin{pmatrix} I & A_d^{-1}G^T & 0 \\ 0 & I & -S_1^{-1}B^T \\ 0 & 0 & I \end{pmatrix}}_{U}$$

$$= \underbrace{\begin{pmatrix} A_d & 0 & 0 \\ G & -S_1 & 0 \\ 0 & B & S_2 \end{pmatrix}}_{LD} \underbrace{\begin{pmatrix} I & A_d^{-1}G^T & 0 \\ 0 & I & -S_1^{-1}B^T \\ 0 & 0 & I \end{pmatrix}}_{U},$$

where

(4.2)
$$S_1 = A_s + GA_d^{-1}G^T$$

and

(4.3)
$$S_2 = BS_1^{-1}B^T$$

are Schur complements.

In (4.1) we have written two forms of factorizations. The first factorization is a block LDU factorization, where L is unit lower triangular, D is block diagonal, and U is unit upper triangular. The second factorization is a block decomposition where the lower block-triangular matrix is simply the product of LD in the LDU block factorization. We use these forms to consider block preconditioners. The Appendix provides additional options.

Ideal preconditioners we consider and analyze are:

$$\mathcal{M}_1 = \begin{pmatrix} A_d & 0 & 0 \\ 0 & S_1 & 0 \\ 0 & 0 & S_2 \end{pmatrix}, \quad \mathcal{M}_2 = \begin{pmatrix} A_d & 0 & 0 \\ G & S_1 & 0 \\ 0 & 0 & S_2 \end{pmatrix}, \quad \mathcal{M}_3 = \begin{pmatrix} A_d & 0 & 0 \\ G & -S_1 & 0 \\ 0 & B & S_2 \end{pmatrix}.$$

The choice of $\mathcal{M}_1$ is based on the matrix D of the LDU factorization of $\mathcal{K}$. Since $\mathcal{K}$ is nonsymmetric and G is an interface matrix that contains important physical information on the coupling effect between the Stokes and Darcy equations, it seems to make sense to consider block triangular preconditioners that contain G in the (2,1) block. The choice of $\mathcal{M}_2$ amounts to a relatively modest revision of $\mathcal{M}_1$, where the interface matrix G is added as the (2,1) block. The matrix $\mathcal{M}_3$ is equal to LD in (4.1).

Recall from Section 3.5 that if Neumann boundary conditions are considered for the Darcy problem, then the matrix A_d is positive semidefinite with a one-dimensional

null space spanned by the all-ones vector. The singularity presents a challenge for the design of preconditioners, and we do not further pursue this scenario in this paper. As previously mentioned, we focus on Dirichlet boundary conditions, for which A_d is symmetric positive definite and the Schur complements are well defined. The matrix $\mathcal{M}_1$ is symmetric positive definite.

4.1. Spectral analysis. There is an increasing body of literature on symmetric double saddle-point systems. Block diagonal preconditioners have been extensively analyzed [1, 3, 6, 7, 8, 25, 38, 39, 44], including bounds on the eigenvalues and theoretical observations on their algebraic multiplicities. The double saddle-point matrix considered in this paper bears similarities, but it has a few distinct features due to its nonsymmetry.

THEOREM 4.1. *The matrix $\mathcal{M}_1^{-1}\mathcal{K}$ has the following eigenvalues and algebraic multiplicities:*

(i) *1 with multiplicity $n^2 - n$;*

(ii) *-1 with multiplicity $(n-1)^2$;*

(iii) *$\frac{-1 \pm \sqrt{5}}{2}$ with multiplicity $n^2 - n$ for each.*

In addition:

(a) *At most n eigenvalues are larger than 1.*

(b) *At most n eigenvalues are located at $(0,1) \backslash \left\{ \frac{-1+\sqrt{5}}{2} \right\}$.*

Proof. By direct calculation,

$$\mathcal{M}_1^{-1}\mathcal{K} = \begin{pmatrix} I & A_d^{-1}G^T & 0 \\ S_1^{-1}G & -S_1^{-1}A_s & S_1^{-1}B^T \\ 0 & S_2^{-1}B & 0 \end{pmatrix}.$$

Let $\begin{pmatrix} x^T & y^T & z^T \end{pmatrix}^T$ be an eigenvector of $\mathcal{M}_1^{-1}\mathcal{K}$ associated with eigenvalue λ, that is

$$\begin{pmatrix} I & A_d^{-1}G^T & 0 \\ S_1^{-1}G & -S_1^{-1}A_s & S_1^{-1}B^T \\ 0 & S_2^{-1}B & 0 \end{pmatrix} \begin{pmatrix} x \\ y \\ z \end{pmatrix} = \lambda \begin{pmatrix} x \\ y \\ z \end{pmatrix}.$$

We thus have

(4.4a) $$x + A_d^{-1}G^T y = \lambda x,$$

(4.4b) $$S_1^{-1}Gx - S_1^{-1}A_s y + S_1^{-1}B^T z = \lambda y,$$

(4.4c) $$(BS_1^{-1}B^T)^{-1}By = \lambda z.$$

(i) <u>eigenvalue $\lambda = 1$</u>: When $y = z = 0$, (4.4) is reduced to

$$x = \lambda x,$$

$$S_1^{-1}Gx = 0,$$

which means that $\lambda = 1$ is an eigenvalue of $\mathcal{M}_1^{-1}\mathcal{K}$ with $Gx = 0$. Since the null space of G has dimension $n^2 - n$, see (3.10), $\lambda = 1$ is an eigenvalue with multiplicity $n^2 - n$.

(ii) <u>eigenvalue $\lambda = -1$</u>: If $x = z = 0$, then (4.4) is reduced to

(4.5a) $$A_d^{-1}G^T y = 0,$$

(4.5b) $$-S_1^{-1}A_s y = \lambda y,$$

(4.5c) $$By = 0.$$

365 We have $A_s = S_1 - GA_d^{-1}G^T$. Using (4.5a), we rewrite (4.5b) as

366 $$-S_1^{-1}(S_1 - GA_d^{-1}G^T)y = -y + 0 = \lambda y,$$

367 which means that $\lambda = -1$. Next we prove that such $y \neq 0$ exists. From (4.5a) and
368 (3.10), we see that y has the following structure

369 $$y = \begin{pmatrix} y_1 \\ 0 \\ y_2 \end{pmatrix},$$

370 where y_1 and y_2 can have any value, as long as they are not simultaneously zero.
371 Now, we consider (4.5c). Then, y_1, y_2 satisfy $\bar{B}\begin{pmatrix} y_1^T & y_2^T \end{pmatrix}^T = 0$ (see (3.14)). From
372 Lemma 3.2 we know that the nullity of $\bar{B}$ is $(n-1)^2$, which is the multiplicity of the
373 eigenvalue -1.
374
375 (iii) eigenvalues $\lambda = \frac{-1\pm\sqrt{5}}{2}$: If $x = 0, y \neq 0, z \neq 0$, then (4.4) is reduced to

376 (4.6a) $$A_d^{-1}G^T y = 0,$$

377 (4.6b) $$-S_1^{-1}A_s y + S_1^{-1}B^T z = \lambda y,$$

378
379 (4.6c) $$(BS_1^{-1}B^T)^{-1}By = \lambda z.$$

380 Using $A_s = S_1 - GA_d^{-1}G^T$ and (4.6a), we rewrite (4.6b) as

381 $$-S_1^{-1}(S_1 - GA_d^{-1}G^T)y + S_1^{-1}B^T z = -y + S_1^{-1}B^T z = \lambda y,$$

382 which gives $y = \frac{1}{1+\lambda}S_1^{-1}B^T z$. Substituting y into (4.6c) gives

383 $$(BS_1^{-1}B^T)^{-1}By = \frac{1}{1+\lambda}(BS_1^{-1}B^T)^{-1}BS_1^{-1}B^T z = \frac{1}{1+\lambda}z = \lambda z.$$

384 It follows that $\frac{1}{1+\lambda} = \lambda$. Then we have $\lambda = \frac{-1\pm\sqrt{5}}{2}$. From (4.6a) we have $G^T y = 0$,
385 which means we have a set of $n^2 - n$ linearly independent vectors y here. It follows
386 that the pair of eigenvalues $\frac{-1\pm\sqrt{5}}{2}$ have multiplicity $n^2 - n$ each.
387 　　Next, we prove that the number of eigenvalues that satisfy $\lambda > 1$ is at most n.
388 From (4.4a), we have

389 (4.7) $$x = \frac{1}{\lambda - 1}A_d^{-1}G^T y.$$

390 We claim that $G^T y \neq 0$. This can be shown by contradiction, as follows. If $G^T y = 0$,
391 from (4.4a), we would have $x = 0$. At this point, if $z = 0$, then from the proof of
392 (ii) it would follow that $\lambda = -1$, which contradicts our assumption that $\lambda > 1$. So
393 $z \neq 0$. If $y \neq 0$, from the proof of (iii), we would have $\lambda = \frac{-1\pm\sqrt{5}}{2}$, which contradicts
394 our assumption that $\lambda > 1$. So $y = 0$. However, this leads to $z = 0$, which is a
395 contradiction. Thus, $G^T y \neq 0$, that is, $y \notin \ker(G^T)$. Since $\text{rank}(G^T) = n$, there are
396 at most n such linearly independent vectors y. From (4.4c), we have

397 $$z = (\lambda BS_1^{-1}B^T)^{-1}By.$$

398 So the space spanned by the eigenvectors $\begin{pmatrix} x^T & y^T & z^T \end{pmatrix}^T$ has dimension at most n.

Next, we claim that there are n^2 eigenvalues in the interval $(0,1)$. Substituting (4.7) into (4.4b) and solving for y gives

$$y = \left(\frac{1}{1-\lambda} G A_d^{-1} G^T + \lambda S_1 + A_s \right)^{-1} B^T z.$$

Since B^T is full rank, it follows that $z \neq 0$; otherwise, $y = x = 0$. Thus, z is in the range of B^T. Note that B^T has rank n^2. The space spanned by the eigenvectors $\begin{pmatrix} x^T & y^T & z^T \end{pmatrix}^T$ has dimension at most n^2. From (iii), we know that $\frac{-1+\sqrt{5}}{2}$ has multiplicity $n^2 - n$, so the number of eigenvalues in $(0,1)\backslash\{\frac{-1+\sqrt{5}}{2}\}$ is at most $n^2 - (n^2 - n) = n$.   □

Remark 4.2. For symmetric block diagonal preconditioners applied to symmetric double saddle-point systems, spectral studies provide results on the boundedness away from zero of all the eigenvalues of the preconditioned matrices; see, e.g., [6, Theorem 3.3]. In Theorem 4.1 we do not know the location of $2n-1$ of the $4n^2 - n$ eigenvalues.

THEOREM 4.3. *The eigenvalues of* $\mathcal{M}_2^{-1}\mathcal{K}$ *are*
  (i) 1 *with multiplicity* n^2;
  (ii) -1 *with multiplicity* $n^2 - n$;
  (iii) $\frac{-1\pm\sqrt{5}}{2}$ *with multiplicities* n^2 *each.*

Proof. It can be shown that

$$\mathcal{M}_2^{-1} = \begin{pmatrix} A_d^{-1} & 0 & 0 \\ -S_1^{-1}G A_d^{-1} & S_1^{-1} & 0 \\ 0 & 0 & S_2^{-1} \end{pmatrix},$$

and it follows that

$$\mathcal{M}_2^{-1}\mathcal{K} = \begin{pmatrix} I & A_d^{-1}G^T & 0 \\ 0 & -I & S_1^{-1}B^T \\ 0 & S_2^{-1}B & 0 \end{pmatrix}.$$

Let $\begin{pmatrix} x^T & y^T & z^T \end{pmatrix}^T$ be an eigenvector of $\mathcal{M}_2^{-1}\mathcal{K}$ associated with eigenvalue λ, that is,

$$\begin{pmatrix} I & A_d^{-1}G^T & 0 \\ 0 & -I & S_1^{-1}B^T \\ 0 & S_2^{-1}B & 0 \end{pmatrix} \begin{pmatrix} x \\ y \\ z \end{pmatrix} = \lambda \begin{pmatrix} x \\ y \\ z \end{pmatrix}.$$

We rewrite the above as

(4.8a) $x + A_d^{-1}G^T y = \lambda x,$

(4.8b) $-y + S_1^{-1}B^T z = \lambda y,$

(4.8c) $(BS_1^{-1}B^T)^{-1}By = \lambda z.$

It is obvious that $\begin{pmatrix} x^T & y^T & z^T \end{pmatrix}^T = \begin{pmatrix} x^T & 0 & 0 \end{pmatrix}^T$ where $x \neq 0$ is an eigenvector of $\mathcal{M}_2^{-1}\mathcal{K}$ with $\lambda = 1$. Since $x \in \mathbb{R}^{n^2 \times 1}$, we have that $\lambda = 1$ is an eigenvalue with multiplicity n^2.

If $\lambda = -1$ and $y \neq 0$, from (4.8b) we have $S_1^{-1}B^T z = 0$. It follows that $B^T z = 0$. Since B^T has full rank, $z = 0$. From (4.8c), we have $By = 0$. Since $B \in \mathbb{R}^{n^2 \times (2n^2 - n)}$ has rank n^2, the null space of B has dimension $2n^2 - n - n^2 = n^2 - n$.

If $\lambda \neq -1$, from (4.8b) we have $By = \frac{1}{1+\lambda} BS_1^{-1} B^T z$. Using (4.8c), we have $\frac{1}{1+\lambda} z = \lambda z$. Thus, $z \neq 0$ and $\lambda^2 + \lambda - 1 = 0$, that is, $\lambda = \frac{-1 \pm \sqrt{5}}{2}$. Since $z \neq 0 \in \mathbb{R}^{n^2 \times 1}$, the eigenvalue -1 has multiplicity n^2. $\qquad\square$

Finally, the spectrum of the preconditioned matrix associated with $\mathcal{M}_3$ is given as follows.

THEOREM 4.4. *All of the eigenvalues of $\mathcal{M}_3^{-1}\mathcal{K}$ are 1, and the minimal polynomial of this preconditioned matrix is $p(z) = (z-1)^3$.*

Proof. Using the notation of (4.1), the result follows immediately since $\mathcal{M}_3^{-1}\mathcal{K} = (LD)^{-1}LDU = U$. $\qquad\square$

4.2. Approximations of the Schur complements. The choices $\mathcal{M}_1, \mathcal{M}_2$, and $\mathcal{M}_3$ as preconditioners are too computationally costly to work with in practice, so we seek effective approximations. Specifically, in order to make the solver practical, we investigate the structure of the Schur complements S_1 and S_2, and derive approximations that are easier to compute and invert.

4.2.1. Approximations of S_1. To find good approximations of S_1 in (4.2), we seek approximations for the action of its additive components, namely A_s and $GA_d^{-1}G^T$.

Given the sparsity structure of G^T, (3.10), it follows that $GA_d^{-1}G^T$ is given by

$$(4.9) \qquad GA_d^{-1}G^T = \begin{pmatrix} 0 & 0 & 0 \\ 0 & T & 0 \\ 0 & 0 & 0 \end{pmatrix},$$

where T is an $n \times n$ matrix, to be approximated.

Our first (naive) approximation is to take a scaled identity. To that end, we take the diagonal approximation $(\operatorname{diag}(A_d))^{-1} \approx A_d^{-1}$ and ignore the corrections near the boundaries: $T \approx \frac{\tau}{\kappa} I_n$ with $\tau = \frac{1}{3}$, because the diagonal elements of $A_{d,22}$ in (3.8) are $3\kappa/h^2$. The resulting approximation of S_1 is

$$(4.10) \qquad \widetilde{S}_1 = \begin{pmatrix} A_{11} & A_{12} & 0 \\ 0 & A_{22} + \frac{\tau}{\kappa} I_n & A_{23} \\ 0 & A_{32} & A_{33} \end{pmatrix}.$$

In our numerical experiments we have found that this simple approach is effective for a limited range of the physical parameters κ, ν, and h. For a larger range of the parameters it is necessary to consider a more sophisticated alternative, as we do next.

Suppose the Cholesky decomposition of A_d is given by

$$A_d = FF^T,$$

and let $GA_d^{-1}G^T = W^TW$, where $W = F^{-1}G^T$. Taking the block structure of G^T into consideration, we partition F as follows:

$$F = \begin{pmatrix} F_{11} & 0 \\ F_{21} & F_{22} \end{pmatrix},$$

where $F_{11} \in \mathbb{R}^{(n^2-n) \times (n^2-n)}$ and $F_{22} \in \mathbb{R}^{n \times n}$. It readily follows that

$$W = \begin{pmatrix} 0 & 0 & 0 \\ 0 & F_{22}^{-1}/h & 0 \end{pmatrix}$$

and
$$T = (F_{22}^{-T} F_{22}^{-1})/h^2,$$

where F_{22} is an $n \times n$ lower triangular matrix.

In practice, since the Cholesky factorization is too expensive to compute, we compute an incomplete Cholesky factorization of A_d with a moderate drop tolerance. We then replace F_{22} by the corresponding incomplete factor, which we denote by $\tilde{F}_{22}$.

Using the above approach, we denote the corresponding approximation to S_1 as

(4.11)
$$\widehat{S}_1 = \begin{pmatrix} A_{11} & A_{12} & 0 \\ 0 & A_{22} + (\tilde{F}_{22}^{-T} \tilde{F}_{22}^{-1})/h^2 & A_{23} \\ 0 & A_{32} & A_{33} \end{pmatrix}.$$

We stress again that the second block-row has only n rows, and therefore the inversion operations involved in the $(2, 2)$ block are not computationally costly with respect to the overall computational cost of the numerical solution scheme. We have found this approach to be robust with respect to a large range of κ, ν, and h; see Section 5.

4.2.2. Approximation of S_2. Recall from (4.3) that $S_2 = BS_1^{-1}B^T$. Consider $\tilde{S}_1$ of (4.10), and let us further sparsify it as follows: we keep the block diagonal part of $\tilde{S}_1$ and A_{23}, which contains important information about the interface, and drop the off-diagonal blocks A_{12} and A_{32}. We further replace the $(2, 2)$ block of the approximation $\tilde{S}_1$ by its diagonal part:

$$\tilde{A}_{22} = \frac{2\nu}{h^2} I_n + \frac{\tau}{\kappa} I_n.$$

We then use this as a sparser approximation of S_1:

$$\check{S}_1 = \begin{pmatrix} A_{11} & 0 & 0 \\ 0 & \tilde{A}_{22} & A_{23} \\ 0 & 0 & A_{33} \end{pmatrix}.$$

Then we have

$$B\check{S}_1^{-1}B^T \approx \begin{pmatrix} B_x & B_0 & B_y \end{pmatrix} \begin{pmatrix} A_{11}^{-1} & 0 & 0 \\ 0 & \tilde{A}_{22}^{-1} & -\tilde{A}_{22}^{-1} A_{23} A_{33}^{-1} \\ 0 & 0 & A_{33}^{-1} \end{pmatrix} \begin{pmatrix} B_x^T \\ B_0^T \\ B_y^T \end{pmatrix}$$

$$= B_x A_{11}^{-1} B_x^T + B_y A_{33}^{-1} B_y^T + B_0 \tilde{A}_{22}^{-1} B_0^T - B_0 \tilde{A}_{22}^{-1} A_{23} A_{33}^{-1} B_y^T.$$

The matrix $B_x A_{11}^{-1} B_x^T + B_y A_{33}^{-1} B_y^T$ can be approximated by a scaled identity, since in the MAC discretization we have that $B_x B_x^T$ and $B_y B_y^T$ are scaled second-derivative operators in each of the variables. In fact,

$$B_x A_{11}^{-1} B_x^T + B_y A_{33}^{-1} B_y^T \approx \frac{1}{\nu} I_{n^2-n}.$$

Then,

$$B_0 \tilde{A}_{22}^{-1} B_0^T = \begin{pmatrix} I_n/h \\ 0 \end{pmatrix} \left(\frac{2\nu}{h^2} I_n + \frac{\tau}{\kappa} I_n \right)^{-1} \begin{pmatrix} I_n/h & 0 \end{pmatrix} = \begin{pmatrix} \frac{\kappa}{2\nu\kappa + h^2\tau} I_n & 0 \\ 0 & 0 \end{pmatrix}.$$

TABLE 1
Values of n and the dimensions of the corresponding linear systems

n	dimensions
32	4,064
64	16,320
128	65,508
256	261,888
512	1,048,064
1024	4,193,280

Further, we have

$$B_0 \widetilde{A}_{22}^{-1} A_{23} A_{33}^{-1} B_y^T = \begin{pmatrix} I_n/h \\ 0 \end{pmatrix} \left(\frac{2\nu}{h^2} I_n + \frac{\tau}{\kappa} I_n \right)^{-1} \begin{pmatrix} -\frac{2\nu}{h^2} I_n & 0 \end{pmatrix} A_{33}^{-1} B_y^T$$

$$= \begin{pmatrix} -\frac{2\nu\kappa}{h(2\nu\kappa + h^2\tau)} I_n & 0 \\ 0 & 0 \end{pmatrix} A_{33}^{-1} B_y^T.$$

This matrix contains entries that are smaller by a factor of h than $B_0 \widetilde{A}_{22}^{-1} B_0^T$ and therefore we drop it and do not incorporate it into the approximation.

Based on the above, we approximate S_2 by

(4.12) $$\widehat{S}_2 = \frac{1}{\nu} I_{n^2-n} + \begin{pmatrix} \frac{\kappa}{2\nu\kappa + h^2\tau} I_n & 0 \\ 0 & 0 \end{pmatrix} = \begin{pmatrix} \frac{3\nu\kappa + h^2\tau}{\nu(2\nu\kappa + h^2\tau)} I_n & 0 \\ 0 & \frac{1}{\nu} I_{n^2-2n} \end{pmatrix}.$$

4.2.3. Practical block preconditioners. Based on the discussion in Subsections 4.2.1 and 4.2.2, for our numerical experiments we will consider mostly the following block preconditioners:

$$\widehat{\mathcal{M}}_1 = \begin{pmatrix} A_d & 0 & 0 \\ 0 & -\widehat{S}_1 & 0 \\ 0 & 0 & \widehat{S}_2 \end{pmatrix}, \quad \widehat{\mathcal{M}}_2 = \begin{pmatrix} A_d & 0 & 0 \\ G & -\widehat{S}_1 & 0 \\ 0 & 0 & \widehat{S}_2 \end{pmatrix}, \quad \widehat{\mathcal{M}}_3 = \begin{pmatrix} A_d & 0 & 0 \\ G & -\widehat{S}_1 & 0 \\ 0 & B & \widehat{S}_2 \end{pmatrix},$$

where $\widehat{S}_1$ and $\widehat{S}_2$ are given by (4.11) and (4.12), respectively.

5. Numerical experiments. We consider three numerical examples. The first two are taken from [43], but with a different formulation of the BJS condition. We use those examples to perform an error validation and confirm that we observe the expected order of the error. These two examples impose specific constraints on the values of the physical parameters ν, κ.

We then move to consider a third example from [31], where there is no restriction on the physical parameters; this allows us to investigate the convergence behavior of our solver for a broad range of the parameters. As explained in Section 4, we assume Dirichlet boundary conditions in all our examples. Our code is written in MATLAB. As such, it is not optimized to maximize computational efficiency.

The dimensions of the linear systems used in our numerical experiments are given in Table 1.

Example 1: We take $\Omega_s = [0,1] \times [1,2]$ and $\Omega_d = [0,1] \times [0,1]$. The analytical

solution is given by

$$u = -\frac{1}{\pi}e^y \sin(\pi x),$$

$$v = (e^y - e)\cos(\pi x),$$

$$p = 2e^y \cos(\pi x),$$

$$\phi = (e^y - ye)\cos(\pi x).$$

The interface equations (2.5) require that $\alpha = \nu = 1$.

Example 2: We consider $\Omega_s = [0,1] \times [1,2]$ and $\Omega_d = [0,1] \times [0,1]$. The analytical solution is given by

$$u = (y-1)^2 + x(y-1) + 3x - 1,$$

$$v = x(x-1) - 0.5(y-1)^2 - 3y + 1,$$

$$p = 2x + y - 1,$$

$$\phi = x(1-x)(y-1) + \frac{(y-1)^3}{3} + 2x + 2y + 4.$$

By (2.5) it is required that $\alpha = \nu = \kappa = 1$.

Example 3: We consider $\Omega_s = [0,1] \times [0,1]$ and $\Omega_d = [0,1] \times [-1,0]$. The equation is constructed so that the analytical solution is given by

$$u = \eta'(y)\cos x,$$

$$v = \eta(y)\sin x,$$

$$p = 0,$$

$$\phi = e^y \sin x,$$

where

$$\eta(y) = -\kappa - \frac{y}{2\nu} + \left(-\frac{\alpha}{4\nu^2} + \frac{\kappa}{2}\right)y^2.$$

Using interface condition (2.5a), there is no constraint on κ. Using interface condition (2.5b), there is no constraint on ν. Using interface condition (2.5c), there is no constraint on α and ν.

5.1. Convergence order study. First, we check the convergence order of the velocity and pressure for the three examples.

Example 1: Table 2 shows the convergence rates for the values of the physical parameters $\alpha = \nu = \kappa = 1$. We observe second-order convergence for the velocity and pressure components for Stokes, while for the Darcy the convergence order of ϕ is slightly lower than 2.

Example 2: Table 3 shows the convergence rates for the values of the physical parameters $\alpha = \nu = \kappa = 1$. We observe second-order convergence for the pressure components of Stokes and first-order convergence for the remaining components.

Example 3: Table 4 shows the convergence rates for $\nu = 1$ and $\kappa = 10^{-2}$, where we observe first-order convergence for all components. This is typical for most values of the physical parameters that we have tested. As an illustration of the quality of the solution, the error norms at the finest level of the discretization (512×512 grid) for $u, v, p,$ and ϕ were computed to be, respectively, 5.5027×10^{-6}, 6.3298×10^{-6},

TABLE 2
Convergence rates for Example 1. Each row shows the ratio between error norms for two adjacent grids.

n_1/n_2	32/64	64/128	128/256	256/512
u	1.9888	1.9957	1.9983	1.9994
v	1.9895	1.9965	1.9990	1.9998
p	1.9946	1.9982	1.9994	1.9998
ϕ	1.7136	1.7759	1.8198	1.8514

TABLE 3
Convergence rates for Example 2. Each row shows the ratio between error norms for two adjacent grids.

n_1/n_2	32/64	64/128	128/256	256/512
u	1.9070	1.7649	1.4823	1.2078
v	2.0639	1.9929	1.5441	1.0405
p	2.0035	2.0197	2.0306	2.0009
ϕ	1.0139	1.0072	1.0036	1.0018

8.9076×10^{-4}, and 5.8343×10^{-5}. We note that for $\nu = \kappa = 1$ we have observed nearly second-order convergence rates for all components.

In summary, in all examples we observe either first or second-order convergence, depending on the values of the physical parameters and the model problems. This is in line with or better than the theoretically-guaranteed first-order convergence [43]. We also note that although the values of the meshsize h used in our tests do not always satisfy (3.1), the scheme still converges and we obtain the theoretically-guaranteed first-order convergence.

In the remainder of this section we conduct our numerical tests using Example 3.

5.2. Eigenvalue distribution of the double saddle-point matrix (Example 3). We explore the effect of κ and ν on the eigenvalue distribution of $\mathcal{K}$ for Example 3. We take $n = 32$ and vary the values of κ and ν. The results are shown in Figure 6. Notice that in all examples, the magnitudes of the real parts of the eigenvalues are significantly larger than the magnitudes of the imaginary parts.

We observe that for $\nu = \kappa = 1$ (top left plot) the real part of the eigenvalues is spread rather evenly (in terms of magnitudes) over both sides of the real axis. We also notice that the eigenvalues with a negative real part are complex, whereas the eigenvalues on the right half of the plane are real. While the imaginary parts of the eigenvalues do not exceed approximately 2.5, the largest positive and negative real parts are almost 10^4 in value.

Taking $\kappa = 0.01$ and keeping $\nu = 1$ (top right plot) generates a rather dramatic effect on the real part of the eigenvalues; they are shifted towards the negative axis. In our computations we have found that the eigenvalue with the algebraically maximal real part was approximately equal to 81.9, whereas the eigenvalue with the algebraically minimal real part was approximately $-8,183.0$.

Taking $\kappa = 1$ and $\nu = 0.01$ (bottom left plot) shifts the real parts of the eigenvalues to be mostly positive. The scales of the imaginary parts are now smaller. The algebraically smallest eigenvalue in this case was -0.4 and the algebraically largest eigenvalue was approximately $8,189.5$.

Finally, we show the interesting case where $\nu = 10^{-4}$ and $\kappa = 10^{-8}$ (bottom right

TABLE 4
Convergence rates for Example 3 with $\nu = 1$ and $\kappa = 10^{-2}$. Each row shows the ratio between error norms for two adjacent grids.

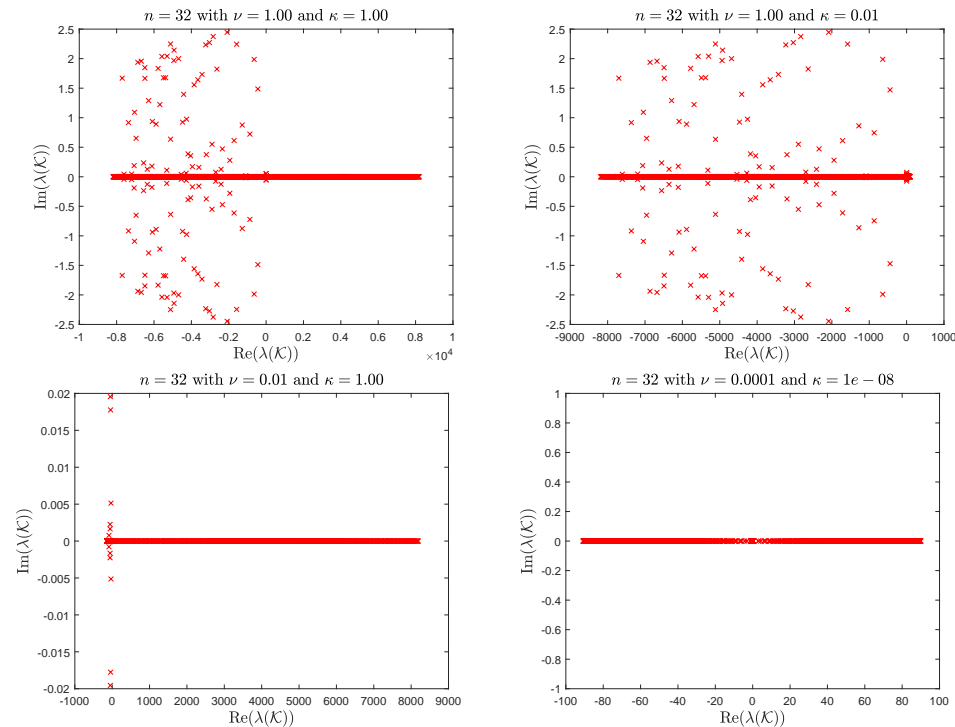| n_1/n_2	32/64	64/128	128/256	256/512
u	1.0386	1.0158	1.0065	1.0027
v	1.0940	1.0458	1.0224	1.0110
p	1.0767	1.0351	1.0165	1.0079
ϕ	0.9750	0.9872	0.9935	0.9968

FIG. 6. *The eigenvalue distribution of $\mathcal{K}$ with different values of ν and κ.*

plot). All eigenvalues in this case are real and are spread over both axes in a rather symmetrical fashion. The algebraically maximal value in this case was 90.0 and the algebraically minimal one was -90.8.

The above observations indicate that the spectral properties of the coefficient matrix highly depend on the values of the physical parameters κ and ν.

5.3. GMRES performance. In our numerical tests we run GMRES(20) and stop the iteration once the initial relative residual is reduced by a factor of 10^{-8} or a maximum iteration count of 500 iterations has been reached. For the incomplete Cholesky factorization of the Schur complement S_1, we use a drop tolerance of 10^{-2}.

In Table 5 we report the iteration counts of preconditioned GMRES using preconditioners $\widehat{\mathcal{M}}_1$ and $\widehat{\mathcal{M}}_2$. We see that these two preconditioners scale poorly with respect to small physical parameters. To better understand this behavior, we explore an improved version of the preconditioner, where we use the approximation $\widehat{S}_1$ and exact S_2 for the Schur complements in $\mathcal{M}_1$ and $\mathcal{M}_2$; we refer to the correspond-

ing preconditioners as $\mathcal{M}_{1,in}$ and $\mathcal{M}_{2,in}$, where the subscript 'in' is shorthand for 'inexact.' We report the corresponding results in Table 6. We see a much better performance. However, the cost of inverting S_2 exactly is too high in practice, and we seek less costly alternatives. We thus consider approximations of $\mathcal{M}_3$: we use the simple approximations $\hat{S}_1$ and $\hat{S}_2$ defined in (4.11) and (4.12), respectively, and include the block B. This is the preconditioning approach that we have found to be the most effective.

TABLE 5

Iteration counts of GMRES(20) for the preconditioners $\widehat{\mathcal{M}}_1$ and $\widehat{\mathcal{M}}_2$ with $\nu = 1$ and varying n and κ. The symbol '-' marks no convergence to a relative residual tolerance of 10^{-8} within 500 iterations. The two schemes failed to converge for $\kappa < 10^{-4}$.

n	$\widehat{\mathcal{M}}_1$			$\widehat{\mathcal{M}}_2$		
κ	32	64	128	32	64	128
10^0	60	62	60	55	57	62
10^{-1}	67	75	87	62	64	70
10^{-2}	186	215	275	67	125	114
10^{-3}	-	-	-	99	159	204
10^{-4}	444	285	-	239	78	-
10^{-5}	-	-	-	-	-	-

TABLE 6

Iteration counts of GMRES(20) for the inexact versions $\mathcal{M}_{1,in}$ and $\mathcal{M}_{2,in}$ corresponding to preconditioners $\mathcal{M}_1$ and $\mathcal{M}_2$ with $\nu = 1$ and varying n and κ, using approximation $\hat{S}_1$ and the exact S_2.

n	$\mathcal{M}_{1,in}$		$\mathcal{M}_{2,in}$	
κ	32	64	32	64
10^0	14	15	10	11
10^{-1}	17	19	12	14
10^{-2}	25	26	15	16
10^{-3}	33	35	17	21
10^{-4}	34	40	17	21
10^{-5}	29	38	16	21
10^{-6}	24	34	15	19
10^{-7}	25	31	15	17
10^{-8}	22	31	14	18

As per Theorem 4.4, the preconditioned matrix $\mathcal{M}_3^{-1}\mathcal{K}$ has one eigenvalue 1 with a minimal polynomial of degree 3. We have confirmed for this ideal (yet impractical) preconditioner that GMRES takes three iterations to converge.

In the experiments reported henceforth, we use the approximation $\hat{S}_2$ in (4.12) for S_2; we have found this approximation to be robust with respect to the physical parameters. On the other hand, the quality of the approximation of S_1 has a more dramatic effect on convergence of GMRES, as we discuss below. We consider approximations of S_1, which result in inexact versions of $\mathcal{M}_1, \mathcal{M}_2$ and $\mathcal{M}_3$.

In Table 7 we show that the approximation of S_1 based on the scaled identity approximation of T, namely $\tilde{S}_1$ given in (4.10), is only effective for relatively large values of ν and κ. We set $\nu = 1$ and observe a good degree of scalability (nearly constant iteration counts) for $\kappa = 1$ and $\kappa = 0.1$, but convergence starts degrading

TABLE 7

Iteration counts of GMRES(20) with an inexact version of $\mathcal{M}_3$, using $\hat{S}_2$ and a scaled identity approximation of S_1 with $\nu = 1$ and varying n and κ. The symbol '-' marks no convergence to a relative residual tolerance of 10^{-8} within 500 iterations.

n \ κ	10^0	10^{-1}	10^{-2}	10^{-3}	10^{-4}	10^{-5}	10^{-6}	10^{-7}	10^{-8}
32	18	19	21	37	49	76	79	360	-
64	18	19	24	39	75	-	-	-	-
128	19	20	25	44	280	-	-	-	-
256	20	21	28	44	-	-	-	-	-
512	21	22	31	39	448	105	-	-	-
1024	22	23	31	37	464	300	-	-	-

TABLE 8

Iteration counts of GMRES(20) for the preconditioner $\widehat{\mathcal{M}}_3$ with $\nu = 1$ and varying n and κ.

n \ κ	10^0	10^{-1}	10^{-2}	10^{-3}	10^{-4}	10^{-5}	10^{-6}	10^{-7}	10^{-8}
32	18	17	18	18	18	18	20	21	23
64	19	19	19	20	21	23	24	38	39
128	20	20	20	23	24	35	37	37	38
256	21	22	22	25	37	32	35	37	39
512	22	23	23	36	36	34	38	39	42
1024	24	25	24	39	37	41	59	60	61

for smaller values of κ, with poor convergence for $\kappa \leqslant 10^{-4}$.

In Tables 8 and 9 we consider the much superior approximation of S_1 based on the incomplete Cholesky factorization with drop tolerance 10^{-2}, namely $\hat{S}_1$ defined in (4.11). We see that for both values of ν and varying values of κ, the preconditioner $\widehat{\mathcal{M}}_3$ is quite robust, although convergence degrades as κ becomes smaller. In Table 10 we replace the approximation of $\hat{S}_1$ by the exact S_1, just to confirm that indeed, the source of the decline in performance for small values of κ is related to the quality of the approximation of S_1. We therefore expect that a better approximation, for example an incomplete Cholesky factorization with a tighter drop tolerance, would yield faster convergence in most cases.

Finally, in Table 11 we show that when the difference in scale between ν and κ is smaller, then preconditioned GMRES with $\widehat{\mathcal{M}}_3$ performs remarkably well even when the parameters are small.

6. Concluding remarks. We have considered the MAC discretization of the Stokes–Darcy equations and have designed a robust and scalable preconditioner for the corresponding linear system. Our conclusions are: (i) The MAC discretization gives rise to attractive sparsity patterns of some of the block matrices, which we are able to take advantage of for approximating the Schur complements. (ii) It is crucial to include the coupling equations (interface conditions) in the preconditioner. (iii) The nonsymmetry of the coefficient matrix is mild and it is possible to design a solver based on spectral considerations. The analysis reveals a rich and interesting spectral structure. The inexact block lower triangular preconditioner $\widehat{\mathcal{M}}_3$ seems promising in terms of robustness with respect to the values of the physical parameters. Among its attractive features is our ability to form effective and relatively cheap approximations

TABLE 9

Iteration counts of GMRES(20) for the preconditioner $\widehat{\mathcal{M}}_3$ with $\nu = 10^{-2}$ and varying n and κ.

n \ κ	10^0	10^{-1}	10^{-2}	10^{-3}	10^{-4}	10^{-5}	10^{-6}	10^{-7}	10^{-8}
32	16	15	16	16	17	19	20	37	39
64	17	16	17	18	20	21	35	36	38
128	18	18	18	11	21	32	33	35	37
256	18	20	21	11	11	11	11	11	11
512	20	30	14	13	12	12	11	11	11
1024	20	32	16	14	13	13	12	12	12

TABLE 10

Iteration counts of GMRES(20) for the inexact version of preconditioner $\mathcal{M}_3$ with $\nu = 10^{-2}$ and varying n and κ, using the exact S_1 and approximation $\hat{S}_2$.

n \ κ	10^0	10^{-1}	10^{-2}	10^{-3}	10^{-4}	10^{-5}	10^{-6}	10^{-7}	10^{-8}
32	14	14	15	15	16	17	19	20	22
64	14	14	15	15	15	17	19	20	31
128	14	14	14	7	15	16	18	20	37

of the Schur complements S_1 and S_2.

REFERENCES

[1] F. ALI BEIK AND M. BENZI, *Iterative methods for double saddle point systems*, SIAM Journal on Matrix Analysis and Applications, 39 (2018), pp. 902–921.

[2] I. BABUŠKA AND G. N. GATICA, *A residual-based a posteriori error estimator for the Stokes–Darcy coupled problem*, SIAM Journal on Numerical Analysis, 48 (2010), pp. 498–523.

[3] A. BEIGL, J. SOGN, AND W. ZULEHNER, *Robust preconditioners for multiple saddle point problems and applications to optimal control problems*, SIAM Journal on Matrix Analysis and Applications, 41 (2020), pp. 1590–1615.

[4] F. P. A. BEIK AND M. BENZI, *Preconditioning techniques for the coupled Stokes–Darcy problem: spectral and field-of-values analysis*, Numerische Mathematik, 150 (2022), pp. 257–298.

[5] C. BERNARDI, T. C. REBOLLO, F. HECHT, AND Z. MGHAZLI, *Mortar finite element discretization of a model coupling Darcy and Stokes equations*, ESAIM: Mathematical Modelling and Numerical Analysis, 42 (2008), pp. 375–410.

[6] S. BRADLEY AND C. GREIF, *Eigenvalue bounds for double saddle-point systems*, IMA Journal on Numerical Analysis, (2022).

[7] M. CAI, G. JU, AND J. LI, *Schur complement based preconditioners for twofold and block tridiagonal saddle point problems*, (2021). https://arxiv.org/abs/2108.08332.

[8] M. CAI, M. MU, AND J. XU, *Preconditioning techniques for a mixed Stokes/Darcy model in porous media applications*, Journal of Computational and Applied Mathematics, 233 (2009), pp. 346–355.

[9] A. CAIAZZO, V. JOHN, AND U. WILBRANDT, *On classical iterative subdomain methods for the Stokes–Darcy problem*, Computational Geosciences, 18 (2014), pp. 711–728.

[10] Y. CAO, M. GUNZBURGER, F. HUA, AND X. WANG, *Coupled Stokes-Darcy model with beavers-joseph interface boundary condition*, Communications in Mathematical Sciences, 8 (2010), pp. 1–25.

[11] L. CHEN, *Finite difference method for Stokes equations: MAC scheme*, (2016).

[12] W. CHEN, F. WANG, AND Y. WANG, *Weak Galerkin method for the coupled Darcy–Stokes flow*,

TABLE 11

Iteration counts of GMRES(20) for the preconditioner $\widehat{\mathcal{M}}_3$ with $\nu = 10^{-4}$ and varying n and κ.

n \ κ	10^0	10^{-1}	10^{-2}	10^{-3}	10^{-4}	10^{-5}	10^{-6}	10^{-7}	10^{-8}
32	9	8	7	7	7	7	7	7	7
64	9	8	6	6	6	6	6	6	6
128	10	7	6	6	6	6	6	6	6
256	11	8	6	6	6	6	6	6	6
512	12	9	7	6	6	6	6	6	6
1024	14	9	7	6	5	5	5	5	5

IMA Journal of Numerical Analysis, 36 (2016), pp. 897–921.

[13] P. CHIDYAGWAI, S. LADENHEIM, AND D. B. SZYLD, *Constraint preconditioning for the coupled Stokes–Darcy system*, SIAM Journal on Scientific Computing, 38 (2016), pp. A668–A690.

[14] M. DISCACCIATI, A. QUARTERONI, ET AL., *Navier-Stokes/Darcy coupling: modeling, analysis, and numerical approximation*, Rev. Mat. Complut, 22 (2009), pp. 315–426.

[15] M. DISCACCIATI, A. QUARTERONI, AND A. VALLI, *Robin–robin domain decomposition methods for the Stokes–Darcy coupling*, SIAM Journal on Numerical Analysis, 45 (2007), pp. 1246–1268.

[16] T. DURETZ, D. A. MAY, T. GERYA, AND P. TACKLEY, *Discretization errors and free surface stabilization in the finite difference and marker-in-cell method for applied geodynamics: A numerical study*, Geochemistry, Geophysics, Geosystems, 12 (2011).

[17] R. EYMARD, T. GALLOUËT, R. HERBIN, AND J.-C. LATCHÉ, *Convergence of the MAC scheme for the compressible Stokes equations*, SIAM Journal on Numerical Analysis, 48 (2010), pp. 2218–2246.

[18] G. FU AND C. LEHRENFELD, *A strongly conservative hybrid DG/mixed FEM for the coupling of Stokes and Darcy flow*, Journal of Scientific Computing, 77 (2018), pp. 1605–1620.

[19] V. GIRAULT AND H. LOPEZ, *Finite-element error estimates for the MAC scheme*, IMA J. Numer. Anal., 16 (1996), pp. 347–379.

[20] H. HAN AND X. WU, *A new mixed finite element formulation and the MAC method for the Stokes equations*, SIAM J. Numer. Anal., 35 (1998), pp. 560–571.

[21] F. H. HARLOW AND J. E. WELCH, *Numerical calculation of time-dependent viscous incompressible flow of fluid with free surface*, The physics of fluids, 8 (1965), pp. 2182–2189.

[22] P. HESSARI, *Pseudospectral least squares method for Stokes–Darcy equations*, SIAM Journal on Numerical Analysis, 53 (2015), pp. 1195–1213.

[23] K. E. HOLTER, M. KUCHTA, AND K.-A. MARDAL, *Robust preconditioning for coupled Stokes–Darcy problems with the Darcy problem in primal form*, Computers & Mathematics with Applications, 91 (2021), pp. 53–66.

[24] Y. HOU AND Y. QIN, *On the solution of coupled Stokes/Darcy model with Beavers–Joseph interface condition*, Computers & Mathematics with Applications, 77 (2019), pp. 50–65.

[25] N. HUANG AND C.-F. MA, *Spectral analysis of the preconditioned system for the 3 × 3 block saddle point problem*, Numer. Algorithms, 81 (2019), p. 421–444.

[26] T. KARPER, K.-A. MARDAL, AND R. WINTHER, *Unified finite element discretizations of coupled Darcy–Stokes flow*, Numerical Methods for Partial Differential Equations: An International Journal, 25 (2009), pp. 311–326.

[27] D. E. KEYES, L. C. MCINNES, C. WOODWARD, W. GROPP, E. MYRA, M. PERNICE, J. BELL, J. BROWN, A. CLO, J. CONNORS, ET AL., *Multiphysics simulations: Challenges and opportunities*, The International Journal of High Performance Computing Applications, 27 (2013), pp. 4–83.

[28] M.-C. LAI, M.-C. SHIUE, AND K. C. ONG, *A simple projection method for the coupled Navier-Stokes and Darcy flows*, Computational Geosciences, 23 (2019), pp. 21–33.

[29] W. J. LAYTON, F. SCHIEWECK, AND I. YOTOV, *Coupling fluid flow with porous media flow*, SIAM Journal on Numerical Analysis, 40 (2002), pp. 2195–2218.

[30] J.-G. LIU AND W.-C. WANG, *An energy-preserving MAC–Yee scheme for the incompressible MHD equation*, Journal of Computational Physics, 174 (2001), pp. 12–37.

[31] P. LUO, C. RODRIGO, F. J. GASPAR, AND C. W. OOSTERLEE, *Uzawa smoother in multigrid for the coupled porous medium and Stokes flow system*, SIAM Journal on Scientific Computing, 39 (2017), pp. S633–S661.

[32] K. A. MARDAL, X.-C. TAI, AND R. WINTHER, *A robust finite element method for Darcy–Stokes flow*, SIAM Journal on Numerical Analysis, 40 (2002), pp. 1605–1631.

[33] A. MÁRQUEZ, S. MEDDAHI, AND F.-J. SAYAS, *Strong coupling of finite element methods for the Stokes–Darcy problem*, IMA Journal of Numerical Analysis, 35 (2015), pp. 969–988.

[34] S. MCKEE, M. F. TOMÉ, J. A. CUMINATO, A. CASTELO, AND V. G. FERREIRA, *Recent advances in the marker and cell method*, Archives of computational methods in engineering, 11 (2004), pp. 107–142.

[35] S. MCKEE, M. F. TOMÉ, V. G. FERREIRA, J. A. CUMINATO, A. CASTELO, F. SOUSA, AND N. MANGIAVACCHI, *The MAC method*, Computers & Fluids, 37 (2008), pp. 907–930.

[36] M. MU AND J. XU, *A two-grid method of a mixed Stokes–Darcy model for coupling fluid flow with porous media flow*, SIAM Journal on Numerical Analysis, 45 (2007), pp. 1801–1813.

[37] R. A. NICOLAIDES, *Analysis and convergence of the MAC scheme. I. the linear problem*, SIAM Journal on Numerical Analysis, 29 (1992), pp. 1579–1591.

[38] J. W. PEARSON AND A. POTSCHKA, *On symmetric positive definite preconditioners for multiple saddle-point systems*, (2021). https://arxiv.org/abs/2106.12433v3.

[39] ———, *A preconditioned inexact active-set method for large-scale nonlinear optimal control problems*, (2021). https://arxiv.org/abs/2112.05020.

[40] B. RIVIÈRE AND I. YOTOV, *Locally conservative coupling of Stokes and Darcy flows*, SIAM Journal on Numerical Analysis, 42 (2005), pp. 1959–1977.

[41] H. RUI AND Y. SUN, *A MAC scheme for coupled Stokes–Darcy equations on non-uniform grids*, Journal of Scientific Computing, 82 (2020), pp. 1–29.

[42] J. SCHMALFUSS, C. RIETHMÜLLER, M. ALTENBERND, K. WEISHAUPT, AND D. GÖDDEKE, *Partitioned coupling vs. monolithic block-preconditioning approaches for solving Stokes-Darcy systems*, arXiv preprint arXiv:2108.13229, (2021).

[43] M.-C. SHIUE, K. C. ONG, AND M.-C. LAI, *Convergence of the MAC scheme for the Stokes/Darcy coupling problem*, Journal of Scientific Computing, 76 (2018), pp. 1216–1251.

[44] J. SOGN AND W. ZULEHNER, *Schur complement preconditioners for multiple saddle point problems of block tridiagonal form with application to optimization problems*, IMA Journal of Numerical Analysis, 39 (2018), pp. 1328–1359.

[45] Y. SUN AND H. RUI, *Stability and convergence of the mark and cell finite difference scheme for Darcy-Stokes-Brinkman equations on non-uniform grids*, Numerical Methods for Partial Differential Equations, 35 (2019), pp. 509–527.

[46] S. TLUPOVA, *A domain decomposition solution of the Stokes-Darcy system in 3D based on boundary integrals*, Journal of Computational Physics, 450 (2022), p. 110824.

[47] G. WANG, F. WANG, L. CHEN, AND Y. HE, *A divergence free weak virtual element method for the Stokes–Darcy problem on general meshes*, Computer Methods in Applied Mechanics and Engineering, 344 (2019), pp. 998–1020.

[48] S. ZHANG, X. XIE, AND Y. CHEN, *Low order nonconforming rectangular finite element methods for Darcy-Stokes problems*, Journal of Computational Mathematics, (2009), pp. 400–424.

Appendix A. Related block preconditioners. We have considered several additional options for block preconditioners, with some minor changes (e.g., sign changes) in comparison to the ones we have analyzed in Section 4.1:

$$\widetilde{\mathcal{M}}_1 = \begin{pmatrix} A_d & 0 & 0 \\ 0 & -S_1 & 0 \\ 0 & 0 & S_2 \end{pmatrix}, \quad \widetilde{\mathcal{M}}_2 = \begin{pmatrix} A_d & 0 & 0 \\ G & -S_1 & 0 \\ 0 & 0 & S_2 \end{pmatrix}, \quad \widetilde{\mathcal{M}}_3 = \begin{pmatrix} A_d & 0 & 0 \\ G & S_1 & 0 \\ 0 & B & S_2 \end{pmatrix}.$$

We first provide a summary of the eigenvalues of the preconditioned matrices associated with the above preconditioners. The preconditioned matrix $\widetilde{\mathcal{M}}_1^{-1}\mathcal{K}$ has a large number of complex eigenvalues. The preconditioned matrix $\widetilde{\mathcal{M}}_2^{-1}\mathcal{K}$ has three distinct eigenvalues: the eigenvalue 1 with algebraic multiplicity $2n^2 - n$ and the complex eigenvalues $\frac{1 \pm \sqrt{3}i}{2}$ ($i^2 = -1$) with multiplicity n^2 each. Compare this with $\mathcal{M}_2^{-1}\mathcal{K}$, which has four distinct eigenvalues, as per Theorem 4.3. The preconditioned matrix $\widetilde{\mathcal{M}}_3^{-1}\mathcal{K}$ has three distinct eigenvalues: the eigenvalue 1 with algebraic multiplicity n^2, the eigenvalue -1 with algebraic multiplicity $n^2 - n$, and the eigenvalues $\pm\sqrt{2} - 1$ with multiplicities n^2 each. We now prove these results.

THEOREM A.1. *The eigenvalues of $\widetilde{\mathcal{M}}_2^{-1}\mathcal{K}$ are*

  (i) 1 *with multiplicity* $2n^2 - n$*;*

  (ii) $\frac{1 \pm \sqrt{3}i}{2}$ *with multiplicity* n^2 *each.*

  Proof. The preconditioned matrix is given by

$$\widetilde{\mathcal{M}}_2^{-1}\mathcal{K} = \begin{pmatrix} I & A_d^{-1}G^T & 0 \\ 0 & I & -S_1^{-1}B^T \\ 0 & S_2^{-1}B & 0 \end{pmatrix}.$$

Let $\begin{pmatrix} x^T & y^T & z^T \end{pmatrix}^T$ be an eigenvector of $\widetilde{\mathcal{M}}_2^{-1}\mathcal{K}$ associated with eigenvalue λ. We write the corresponding eigenvalue problem as follows:

(A.1a) $$x + A_d^{-1}G^T y = \lambda x,$$

(A.1b) $$y - S_1^{-1}B^T z = \lambda y,$$

(A.1c) $$(BS_1^{-1}B^T)^{-1}By = \lambda z.$$

  Let us consider the vector $\begin{pmatrix} x^T & y^T & z^T \end{pmatrix}^T = \begin{pmatrix} x^T & 0 & 0 \end{pmatrix}^T$, where $x \neq 0$. Then equations (A.1), along with $\lambda = 1$, are satisfied and hence this vector is an eigenvector of $\widetilde{\mathcal{M}}_2^{-1}\mathcal{K}$. Since $x \in \mathbb{R}^{n^2 \times 1}$, 1 is an eigenvalue with multiplicity n^2.

  If $\lambda = 1$ and $y \neq 0$, the three equations of (A.1) are simplified to

(A.2a) $$A_d^{-1}G^T y = 0,$$

(A.2b) $$B^T z = 0,$$

(A.2c) $$By = 0.$$

Since B^T has full rank, (A.2b) leads to $z = 0$. From (A.2c) we have $By = 0$. Since $B \in \mathbb{R}^{n^2 \times (2n^2-n)}$ has rank n^2, the null space of B has dimension $(2n^2-n)-n^2 = n^2-n$. From the proof of Theorem 4.1, y satisfies $G^T y = 0$. Thus, the multiplicity of the eigenvalue 1 with eigenvector $\begin{pmatrix} x^T & y^T & 0 \end{pmatrix}^T$ with $y \neq 0$ is $n^2 - n$. Therefore, 1 has multiplicity $2n^2 - n$.

  If $\lambda \neq 1$, from (A.1b), we have $By = \frac{1}{1-\lambda}BS_1^{-1}B^T z$. Using (A.1c), we have

$$\frac{1}{1 - \lambda}z = \lambda z.$$

Thus, $z \neq 0$ and

$$\lambda^2 - \lambda + 1 = 0,$$

that is $\lambda = \frac{1 \pm \sqrt{3}i}{2}$. Since $z \neq 0 \in \mathbb{R}^{n^2 \times 1}$, the eigenvalues $\frac{1 \pm \sqrt{3}i}{2}$ have multiplicity n^2 each. $\square$

  THEOREM A.2. *The eigenvalues of* $\widetilde{\mathcal{M}}_3^{-1}\mathcal{K}$ *are*

  (i) 1 *with multiplicity* n^2*;*

  (ii) -1 *with multiplicity* $n^2 - n$*;*

  (iii) $\sqrt{2} - 1 \approx 0.4142$ *and* $-\sqrt{2} - 1 \approx -2.4142$ *with multiplicity* n^2 *each.*

  Proof. The preconditioned matrix is given by

$$\widetilde{\mathcal{M}}_3^{-1}\mathcal{K} = \begin{pmatrix} I & A_d^{-1}G^T & 0 \\ 0 & -I & S_1^{-1}B^T \\ 0 & 2S_2^{-1}S_1^{-1} & -I \end{pmatrix}.$$

Thus, n^2 of the eigenvalues of $\widetilde{\mathcal{M}}_3^{-1}\mathcal{K}$ are 1, and the remaining ones are the eigenvalues of

$$H = \begin{pmatrix} -I & S_1^{-1}B^T \\ 2S_2^{-1}S_1^{-1} & -I \end{pmatrix}.$$

We write the corresponding eigenvalue problem for H and obtain

(A.3a) $$-y + S_1^{-1}B^T z = \lambda y,$$

(A.3b) $$2S_2^{-1}By - z = \lambda z.$$

If $\lambda = -1$, then

$$S_1^{-1}B^T z = 0,$$

$$2S_2^{-1}By = 0.$$

Therefore, $B^T z = 0$ and $By = 0$. Since B is full rank, $z = 0$ and y is the null space of B with dimension $(2n^2 - n) - n^2 = n^2 - n$.

If $\lambda \neq -1$, from (A.3a) we have $y = (1 + \lambda)^{-1}S_1^{-1}B^T z$. Therefore $y, z \neq 0$. From (A.3b), we have

$$(1 + \lambda)z = 2S_2^{-1}By = 2S_2^{-1}(1 + \lambda)^{-1}S_1^{-1}B^T z = 2(1 + \lambda)^{-1}z,$$

which gives $(1 + \lambda)^2 = 2$. Therefore $\lambda = \pm\sqrt{2} - 1$. Since B^T has full rank, the eigenvalues $\pm\sqrt{2} - 1$ have multiplicity n^2 each. $\qquad\square$